



Thermoelectric properties of $\text{Bi}_{0.5}\text{Sb}_{1.4-x}\text{Na}_x\text{In}_{0.1}\text{Te}_3$ alloys

Yue-Zhen Jiang, Xing-Kai Duan*

Received: 12 July 2019/Revised: 11 September 2019/Accepted: 15 October 2019/Published online: 14 November 2019
© The Nonferrous Metals Society of China and Springer-Verlag GmbH Germany, part of Springer Nature 2019

Abstract The $\text{Bi}_{0.5}\text{Sb}_{1.4-x}\text{Na}_x\text{In}_{0.1}\text{Te}_3$ ($x = 0.02\text{--}0.20$) alloys were fabricated by high vacuum melting and hot-pressing technique. The phase structures and morphology of the bulk samples were characterized by X-ray diffraction (XRD) and scanning electron microscope (SEM), respectively. Effects of In and Na co-doping on the electrical and thermal transport properties were studied from room temperature to 500 K. Seebeck coefficient of the $\text{Bi}_{0.5}\text{Sb}_{1.5}\text{Te}_3$ can be enhanced by substituting Sb with In and Na at near room temperature. The electrical conductivity of the In and Na co-doped samples is lower than that of the $\text{Bi}_{0.5}\text{Sb}_{1.5}\text{Te}_3$ alloy from room temperature to 500 K. In and Na co-doping of appropriate percentage optimizes the thermal conductivity of the $\text{Bi}_{0.5}\text{Sb}_{1.5}\text{Te}_3$ alloy. The minimum value of thermal conductivity of $\text{Bi}_{0.5}\text{Sb}_{1.36}\text{Na}_{0.04}\text{In}_{0.1}\text{Te}_3$ alloy is $0.45 \text{ W}\cdot\text{m}^{-1}\cdot\text{K}^{-1}$ at 323 K, which leads to a great improvement in the thermoelectric figure of merit (zT). The maximum zT value reaches 1.42 at 323 K.

Keywords Microstructure; Co-doping; Thermal conductivity; Electrical properties

1 Introduction

Thermoelectric materials are used to convert waste heat into electricity or electrical power directly into heating and cooling

[1–5]. Bi_2Te_3 -based alloys are the most important commercial thermoelectric materials near room temperature. Recently, high thermoelectric performance of Bi_2Te_3 -based materials has been achieved by using many methods and strategies such as hot deformation [6–9], point defects [10], nanocomposites [11–13], nanostructures [14–20] and doping [21, 22]. High-efficiency thermoelectric materials require a large Seebeck coefficient, high electrical conductivity and low thermal conductivity. Owing to interdependence of the thermoelectric parameters, increasing the thermoelectric figure of merit (zT) value remains a challenge. It is well known that doping may determine thermoelectric properties of the thermoelectric materials. The alkali atoms tend to have soft rattling-type phonon modes, which results in very low thermal conductivity in Bi_2Te_3 -based materials [23]. Ji et al. [24] had developed a novel alkali metal salt hydrothermal nanocoating treatment method to coat the polycrystalline P-type Bi_2Te_3 bulk grains with a thin layer, and all three constituent physical properties of zT are “decoupled” and can be modified individually by different alkali metal salt solutions. On the other hand, alkali metals doping can effectively improve the Seebeck coefficient. Substituting Ag with Na has great influence on electron band structure and can enhance the Seebeck coefficient effectively, while adding excess Te in Na-doped samples plays a great role in optimizing the electrical and thermal conductivity in AgSbTe_2 compound [25]. Substituting three valence electrons for Sb with five valence electrons in the $\text{Bi}_{0.5}\text{Sb}_{1.5}\text{Te}_3$ alloy can be expected to be beneficial to the optimization of the carrier concentration, which results in an improvement in Seebeck coefficient.

To research the feasibility of the co-doping to enhance thermoelectric properties of the Bi_2Te_3 -based materials, In and Na double partial substitutions for Sb in the $\text{Bi}_{0.5}\text{Sb}_{1.5}\text{Te}_3$ alloys have been done. In present work, the

Y.-Z. Jiang
School of Electronic Engineering, Jiujiang University, Jiujiang
332005, China

X.-K. Duan*
School of Mechanical and Materials Engineering, Jiujiang
University, Jiujiang 332005, China
e-mail: duanxingkai@163.com

samples were prepared by vacuum melting and hot-pressing technique. The effects of In and Na co-doping on electrical and thermal transport properties were investigated.

2 Experimental

Elemental powders with In (99.99%), Bi (99.99%), Sb (99.99%), Te (99.99%) and bulk Na (99.5%) were weighed according to the atomic ratios of $\text{Bi}_{0.5}\text{Sb}_{1.5}\text{Te}_3$, $\text{Bi}_{0.5}\text{Sb}_{1.4-x}\text{Na}_x\text{In}_{0.1}\text{Te}_3$ ($x = 0.02, 0.04, 0.06, 0.08, 0.10, 0.20$). They were charged into a vacuum quartz tube, respectively. The elemental mixtures were melted at 1073 K for 8 h. Then, they were cooled to room temperature in the furnace. The gained ingots were pulverized using the agate mortar in atmosphere environment. The sizes of powders were controlled using the 300-mesh sieve. The powders were hot-pressed in the graphite dies under 50 MPa at 753 K for 1 h. Bulk disk-shaped pellets with dimension of 12 mm \times 2 mm were prepared by hot pressing.

The phase structure and microstructure were analyzed by X-ray diffractometer (XRD, Bruker, D8 Advance with Cu K α radiation, $\lambda = 0.15406$ nm) and scanning electron microscope (SEM, VEGA-II LSU), respectively. The Seebeck coefficients (S) were achieved by testing thermoelectric voltage under a temperature gradient with an accuracy of $\pm 7\%$ from 300 to 500 K. The electrical resistivity (ρ) was measured by four-point probe from 300 to 500 K. The measure error of electrical resistivity is about $\pm 5\%$. The electrical properties were tested perpendicular to the hot-pressing direction. The thermal diffusivity (λ) was tested by the laser flash diffusivity method using a laser flash method (LFA 457). The thermal diffusivity was tested at the parallel to the hot-pressing direction. The measure error of thermal conductivity is about $\pm 5\%$. The heat capacity (C_p) was obtained from differential scanning calorimetry (DSC, DSC-Q20). The thermal conductivity was calculated according to the equation: $\lambda = \kappa/(DC_p)$, where λ is the thermal diffusivity, D is the density of samples, C_p is the heat capacity, and κ is the thermal conductivity. Hall coefficients were measured by the bar method using a Hall measurement system (Accent HL5500PC) at 300 K. The applied magnetic field is perpendicular to the hot-pressing direction.

3 Results and discussion

3.1 Microstructure

XRD patterns of $\text{Bi}_{0.5}\text{Sb}_{1.5}\text{Te}_3$ and $\text{Bi}_{0.5}\text{Sb}_{1.4-x}\text{Na}_x\text{In}_{0.1}\text{Te}_3$ bulk samples are presented in Fig. 1. All the characteristic

peaks of the bulk samples can be indexed into rhombohedral $\text{Bi}_{0.5}\text{Sb}_{1.5}\text{Te}_3$ (JCPDS No. 49-1713) phase with no impurities, which indicates the single-phase structure of the samples. The (00 l) peaks including (006), (009), (0015), (0018) and (0021) can be observed in the diffraction spectrums from section perpendicular to hot-pressing direction, which indicates that the basal planes are preferentially orientated perpendicular to hot-pressing direction. Since the rhombohedral Bi_2Te_3 -based alloys have a quasi-layered crystal structure, it is important to determine whether all the hot-pressed samples are textured or not. The orientation degree of the (00 l) planes can be determined by the orientation factor f , which can be calculated using the following method:

$$f = \frac{P - P_0}{1 - P_0} \quad (1)$$

where P and P_0 are the ratios of the integrated intensities of all (00 l) planes to those of all (hkl) planes for the preferentially oriented and the randomly oriented samples, respectively.

$$P = \frac{I(00l)}{\sum I(hkl)} \quad P_0 = \frac{I_0(00l)}{\sum I_0(hkl)} \quad (2)$$

where $I_0(hkl)$ and $I(hkl)$ are the peak integral intensities for randomly oriented sample and measured samples, respectively. The result of the orientation factor (f) was 0.29 ± 0.01 . Because all the samples were prepared under the same condition, the values of f were almost equal. Therefore, it is concluded that the preferentially oriented c -axis samples can be fabricated by the vacuum melting and hot-pressing method.

SEM images of the $\text{Bi}_{0.5}\text{Sb}_{1.5}\text{Te}_3$ and the $\text{Bi}_{0.5}\text{Sb}_{1.36}\text{Na}_{0.04}\text{In}_{0.1}\text{Te}_3$ samples are shown in Fig. 2. Figure 2a, c shows a laminated structure composed of micro-nanolayers. The $\text{Bi}_{0.5}\text{Sb}_{1.36}\text{Na}_{0.04}\text{In}_{0.1}\text{Te}_3$ sample is found to have some randomly spaced pores in Fig. 2d. The size of these

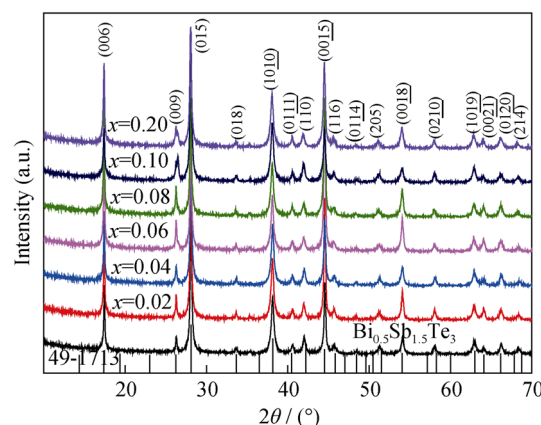


Fig. 1 XRD patterns of $\text{Bi}_{0.5}\text{Sb}_{1.5}\text{Te}_3$ bulk sample and $\text{Bi}_{0.5}\text{Sb}_{1.4-x}\text{Na}_x\text{In}_{0.1}\text{Te}_3$ bulk samples

pores ranges from 300 to 600 nm. The other samples also exhibit the similar microstructures due to the same sintering method, but there are few randomly spaced pores in Fig. 2b. The above results are also confirmed by the density of the samples, which are shown in Table 1. The density of $\text{Bi}_{0.5}\text{Sb}_{1.36}\text{Na}_{0.04}\text{In}_{0.1}\text{Te}_3$ sample is the lowest among all the samples.

3.2 Thermoelectric properties

The temperature dependences of the Seebeck coefficient, the electrical conductivity and the power factor for the samples are shown in Fig. 3. The effects of co-doping on the electrical transport properties of the $\text{Bi}_{0.5}\text{Sb}_{1.4-x}\text{Na}_x\text{In}_{0.1}\text{Te}_3$ ($x = 0.02-0.20$) were systematically investigated. All the samples exhibit the p-type semiconductor behavior within the whole test temperature range, as shown in Fig. 3a. Figure 3a also shows that the In and Na co-doping leads to the increase in the Seebeck coefficient from 300 to 350 K. This is attributed to the In and Na co-doping causing the change in the carrier concentration. As shown in Table 1, the co-doped samples result in the decrease in the hole concentration at room temperature. In this way, the Seebeck coefficients increase. Compared with the $\text{Bi}_{0.5}\text{Sb}_{1.5}\text{Te}_3$ sample, Fig. 3b shows that the electrical conductivity of the In and Na co-doped samples is lower than that of the $\text{Bi}_{0.5}\text{Sb}_{1.5}\text{Te}_3$ alloy within the whole test

Table 1 Density (D), hole concentration (n) and mobility (μ) of bulk $\text{Bi}_{0.5}\text{Sb}_{1.4-x}\text{Na}_x\text{In}_{0.1}\text{Te}_3$ samples at room temperature

Samples	$D/(\text{g}\cdot\text{cm}^{-3})$	$n/(10^{19}\text{ cm}^{-3})$	$\mu/(\text{cm}^2\cdot\text{V}^{-1}\cdot\text{s}^{-1})$
$\text{Bi}_{0.5}\text{Sb}_{1.5}\text{Te}_3$	6.64	1.52	226
$x = 0.02$	6.52	1.05	186
$x = 0.04$	5.98	1.44	186
$x = 0.06$	6.71	0.83	187
$x = 0.08$	6.45	0.92	201
$x = 0.10$	6.53	0.87	206
$x = 0.20$	6.53	0.85	199

temperature range. The carrier concentration and mobility are mainly two factors, which can lead to the differences of the electrical conductivity. The carrier concentration is mainly related to the composition, while the mobility can be affected by the grain size, grain boundary density and defects [26]. The incorporation of In and Na in the structure of $\text{Bi}_{0.5}\text{Sb}_{1.5}\text{Te}_3$ results in the decrease in the hole concentration and mobility in Table 1. Owing to the lower electrical conductivity, the power factors of the co-doped samples are lower slightly than that of the $\text{Bi}_{0.5}\text{Sb}_{1.5}\text{Te}_3$ sample, as shown in Fig. 3c.

The thermal properties and zT values are shown in Fig. 4. As shown in Fig. 4a, the total thermal conductivity

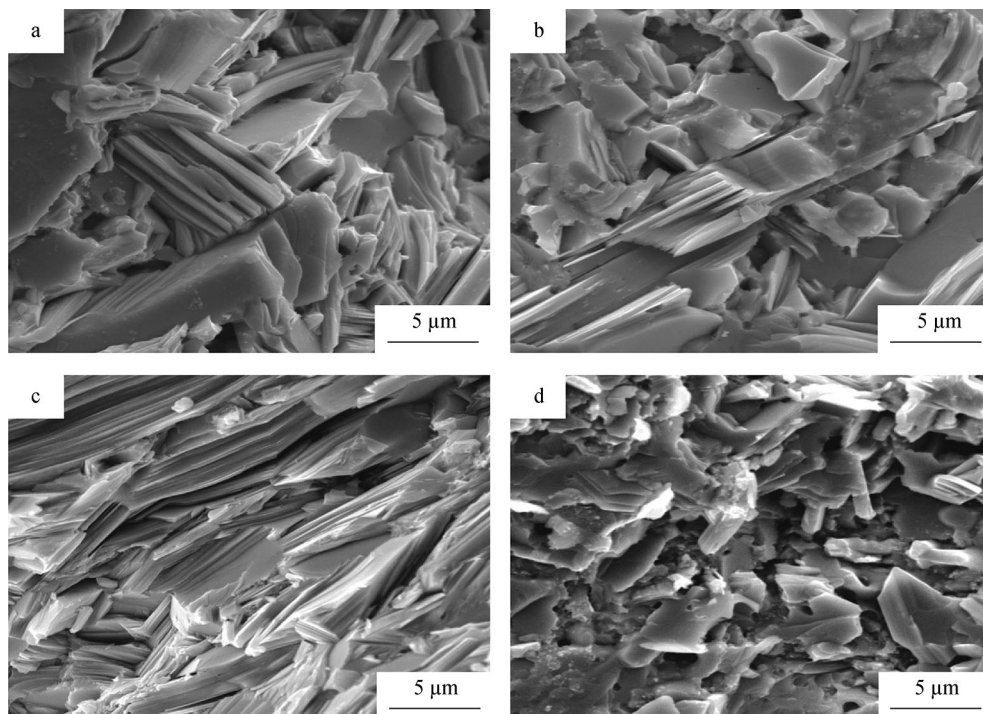


Fig. 2 SEM images of bulk samples: **a** $\text{Bi}_{0.5}\text{Sb}_{1.5}\text{Te}_3$ from sections parallel to hot-pressing direction; **b** $\text{Bi}_{0.5}\text{Sb}_{1.5}\text{Te}_3$ from sections perpendicular to hot-pressing direction; **c** $\text{Bi}_{0.5}\text{Sb}_{1.36}\text{Na}_{0.04}\text{In}_{0.1}\text{Te}_3$ from sections parallel to hot-pressing direction; **d** $\text{Bi}_{0.5}\text{Sb}_{1.36}\text{Na}_{0.04}\text{In}_{0.1}\text{Te}_3$ from sections perpendicular to hot-pressing direction

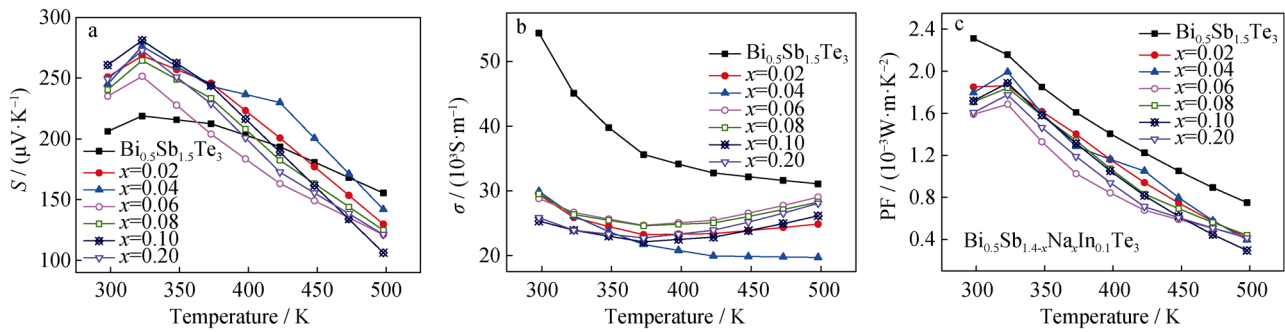


Fig. 3 Temperature dependence of electrical properties of $\text{Bi}_{0.5}\text{Sb}_{1.4-x}\text{Na}_x\text{In}_{0.1}\text{Te}_3$ ($x = 0.02\text{--}0.20$) samples: **a** Seebeck coefficient (S); **b** electrical conductivity (σ); **c** power factor (PF)

is the sum of contributions of the electronic thermal conductivity (κ_e) and the lattice thermal conductivity (κ_L). The electronic thermal conductivity (κ_e) is quantified through the Wiedemann–Franz law: $\kappa_e = L_0 T / \rho$, where L_0 is the Lorenz number, T is the absolute temperature, and ρ is the electrical resistivity [27]. The classical value of the Lorenz number $L_0 = 2.45 \times 10^{-8} \text{ V}^2 \cdot \text{K}^{-2}$ and is valid for a degenerate electron gas. In this paper, $L_0 = 2.0 \times 10^{-8} \text{ V}^2 \cdot \text{K}^{-2}$ is taken, which is used for a heavily doped semiconductor [28]. The total thermal conductivity of the $\text{Bi}_{0.5}\text{Sb}_{1.4-x}\text{Na}_x\text{In}_{0.1}\text{Te}_3$ ($x = 0.02\text{--}0.06$) samples is lower than that of the $\text{Bi}_{0.5}\text{Sb}_{1.5}\text{Te}_3$ sample from 300 to 500 K. The alkali atoms tend to have soft rattling-

type phonon modes, which results in very low thermal conductivity. With the Na substitution fraction increasing from 0.08 to 0.20, the thermal conductivity of the $\text{Bi}_{0.5}\text{Sb}_{1.4-x}\text{Na}_x\text{In}_{0.1}\text{Te}_3$ samples is larger than that of the $\text{Bi}_{0.5}\text{Sb}_{1.5}\text{Te}_3$ sample. Figure 4b shows that the electrical thermal conductivity of the $\text{Bi}_{0.5}\text{Sb}_{1.4-x}\text{Na}_x\text{In}_{0.1}\text{Te}_3$ samples is lower than that of the $\text{Bi}_{0.5}\text{Sb}_{1.5}\text{Te}_3$ sample from 300 to 500 K. The observed decreases are associated with the decrease in the hole concentration and mobility, which are shown in Table 1. As shown in Fig. 4c, the lattice thermal conductivity of the co-doping samples increases with Na substitution fraction increasing from 0.08 to 0.20. Because the electronegativity difference between Na and Te (1.17)

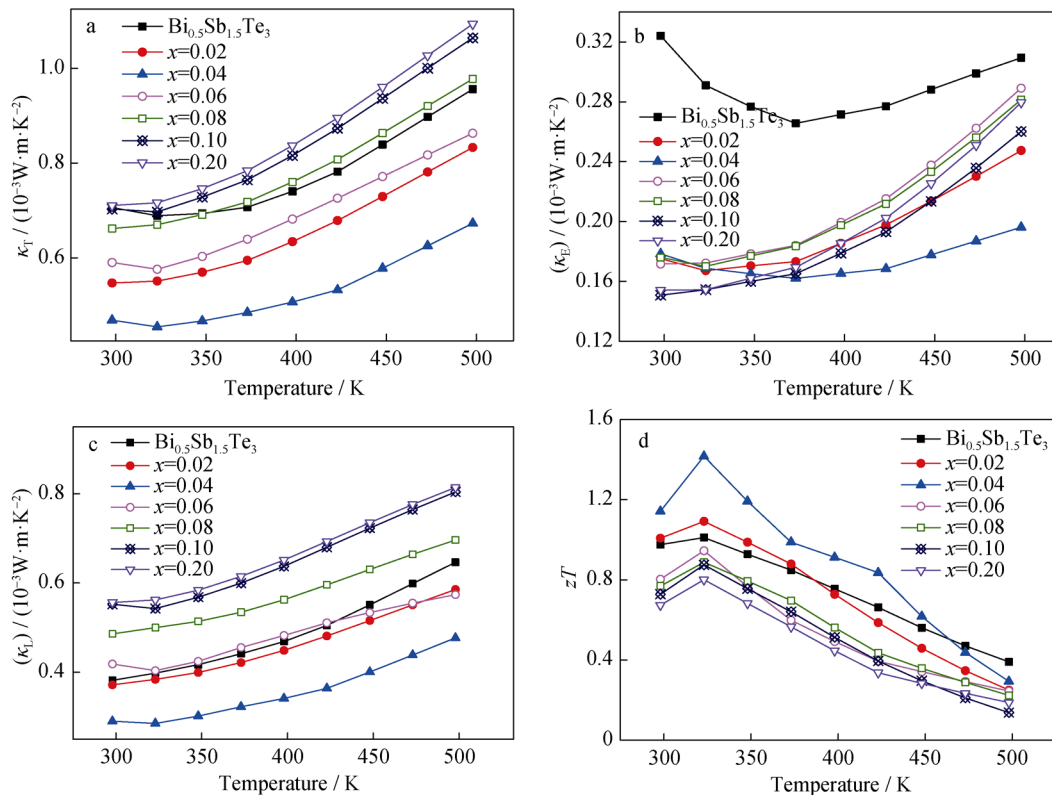


Fig. 4 Temperature dependence of thermal conductivity of $\text{Bi}_{0.5}\text{Sb}_{1.4-x}\text{Na}_x\text{In}_{0.1}\text{Te}_3$ ($x = 0.02\text{--}0.20$) samples: **a** total thermal conductivity (κ_T); **b** electrical thermal conductivity (κ_E); **c** lattice thermal conductivity (κ_L); **d** figure of merit (zT)

is much larger than that between Sb and Te (0.05), replacing Sb with Na should result in much stronger bonding between anions and cations. So, the anharmonicity of the lattice vibrational spectrum is decreased and a rise in κ_L can be expected. With Na substitution fraction increasing from 0.02 to 0.04, the $\text{Bi}_{0.5}\text{Sb}_{1.36}\text{Na}_x\text{In}_{0.1}\text{Te}_3$ samples show lower κ_L over the whole temperature region. The $x = 0.04$ sample has the lowest lattice thermal conductivity. Besides solid solutions scattering high frequency phonons, decrease of the lattice thermal conductivity may be caused by the randomly spaced pores. The spaced pores are shown in Fig. 2d. The randomly spaced pores are beneficial to the scattering of phonons, which contributes to the observed lower lattice thermal conductivity [29–31]. Figure 4d shows temperature dependence of zT value of all the samples. For the $\text{Bi}_{0.5}\text{Sb}_{1.5}\text{Te}_3$ sample, the zT value of 1.01 is obtained at 323 K. Compared with the $\text{Bi}_{0.5}\text{Sb}_{1.5}\text{Te}_3$ sample, the zT values of the $\text{Bi}_{0.5}\text{Sb}_{1.4-x}\text{Na}_x\text{In}_{0.1}\text{Te}_3$ samples decrease with the increasing Na substitution fraction from $x = 0.06$ – 0.2 in the whole temperature range. The $\text{Bi}_{0.5}\text{Sb}_{1.36}\text{Na}_{0.04}\text{In}_{0.1}\text{Te}_3$ sample shows the highest zT values from 300 to 450 K. The increases in zT values can be attributed to the lower thermal conductivity. The zT value of 1.42 is obtained at 323 K. The value represents 40% enhancement with respect to the $\text{Bi}_{0.5}\text{Sb}_{1.5}\text{Te}_3$ sample at the same temperature.

4 Conclusion

XRD results show that all the characteristic peaks of the bulk samples can be indexed into rhombohedral $\text{Bi}_{0.5}\text{Sb}_{1.5}\text{Te}_3$ phase with no impurities. It is concluded that the preferentially oriented c -axis samples can be fabricated by the vacuum melting and hot-pressing method. SEM results show a laminated structure composed of micro-nanolayers. Compared with the $\text{Bi}_{0.5}\text{Sb}_{1.5}\text{Te}_3$ sample, the In and Na co-doped $\text{Bi}_{0.5}\text{Sb}_{1.5}\text{Te}_3$ samples bring about substantial increase in Seebeck coefficient at near room temperature. The electrical conductivity of the In and Na co-doping samples is lower than that of $\text{Bi}_{0.5}\text{Sb}_{1.5}\text{Te}_3$ alloy within the whole test temperature range. For the $\text{Bi}_{0.5}\text{Sb}_{1.36}\text{Na}_{0.04}\text{In}_{0.1}\text{Te}_3$ sample, a minimal thermal conductivity of $0.45 \text{ W}\cdot\text{m}^{-1}\cdot\text{K}^{-1}$ is obtained, with the maximal zT value reaching 1.42 at 323 K. The value represents 40% enhancement with respect to the $\text{Bi}_{0.5}\text{Sb}_{1.5}\text{Te}_3$ alloy at the same temperature. The results show that the In and Na dual substitutions for Sb are effective in enhancing thermoelectric performance of $\text{Bi}_{0.5}\text{Sb}_{1.5}\text{Te}_3$ alloy.

Acknowledgments This study was financially supported by the National Natural Science Foundation of China (No. 51161009).

References

- [1] Zhu TJ. Recent advances in thermoelectric materials and devices. *J Inorg Mater*. 2019;34(3):233.
- [2] Yang L, Chen ZG, Dargusch M, Zou J. High performance thermoelectric materials: progress and their applications. *Adv Energy Mater*. 2018;8:1701797.
- [3] Zhu TJ, Liu YT, Fu CG, Heremans JP, Snyder JG, Zhao XB. Compromise and synergy in high-efficiency thermoelectric materials. *Adv Mater*. 2017;29:1605884.
- [4] Bell LE. Cooling, heating, generating power, and recovering waste heat with thermoelectric systems. *Science*. 2008; 321(5895):1457.
- [5] Hong M, Chen ZG, Yang L, Zou Y, Dargusch M, Wang H, Zou J. Realising zT of 2.3 in p-type $\text{Ge}_{1-x}\text{Sb}_x\text{In}_y\text{Te}$ by reducing the phase-transition temperature and introducing resonant energy doping. *Adv Mater*. 2018;30:1705942.
- [6] Zhai R, Hu L, Wu H, Xu Z, Zhu TJ, Zhao XB. Enhancing thermoelectric performance of n-type hot deformed bismuth-telluride-based solid solutions by nonstoichiometry-mediated intrinsic point defects. *ACS Appl Mater Interfaces*. 2017; 9(34):28577.
- [7] Hu LP, Zhu TJ, Wang YG, Xie HH, Xu ZJ, Zhao XB. Shifting up the optimum figure of merit of p-type bismuth telluride-based thermoelectric materials for power generation by suppressing intrinsic conduction. *NPG Asia Mater*. 2014;6(2):e88.
- [8] Xu ZJ, Hu LP, Ying PJ, Zhao XB, Zhu TJ. Enhanced thermoelectric and mechanical properties of zone melted p-type $(\text{Bi}, \text{Sb})_2\text{Te}_3$ thermoelectric materials by hot deformation. *Acta Mater*. 2015;84:385.
- [9] Xu Z, Wu H, Zhu T, Fu C, Liu X, He J, Zhao X. Attaining high mid-temperature performance in $(\text{Bi}, \text{Sb})_2\text{Te}_3$ thermoelectric materials via synergistic optimization. *NPG Asia Mater*. 2016; 8(9):e302.
- [10] Hu L, Zhu T, Liu X, Zhao X. Point defect engineering of high-performance bismuth-telluride-based thermoelectric materials. *Adv Funct Mater*. 2014;24(33):5211.
- [11] Ajay SN, Zhao YY, Yu LG, Aik Michael KK, Dresselhaus MS, Xiong QH. Enhanced thermoelectric properties of solution grown $\text{Bi}_2\text{Te}_{(3-x)}\text{Se}_{(x)}$ nanoplatelet composites. *Nano Lett*. 2012; 12:1203.
- [12] Cao YQ, Zhao XB, Zhu TJ, Zhang XB, Tu JP. Syntheses and thermoelectric properties of $\text{Bi}_2\text{Te}_3/\text{Sb}_2\text{Te}_3$ bulk nanocomposites with laminated nanostructure. *Appl Phys Lett*. 2008;92(143106): 1.
- [13] Li JH, Tan Q, Li JF, Liu DW, Li F, Li ZY, Zou MM, Wang K. BiSbTe-based nanocomposites with high ZT : the effect of sic nanodispersion on thermoelectric properties. *Adv Funct Mater*. 2013;23(35):4317.
- [14] Chen XZ, Liu LF, Dong Y, Wang LJ, Chen LD, Jiang W. Preparation of nano-sized Bi_2Te_3 thermoelectric material powders by cryogenic grinding. *Prog Nat Sci Mater Int*. 2012;22: 201.
- [15] Xie WJ, Tang XF, Yan YG, Zhang QJ, Tritt TM. Unique nanostructures and enhanced thermoelectric performance of melt-spun BiSbTe alloys. *Appl Phys Lett*. 2009;94(102111):1.
- [16] Li D, Sun RR, Qin XY. Improving thermoelectric properties of p-type Bi_2Te_3 -based alloys by spark plasma sintering. *Prog Nat Sci Mater Int*. 2011;21:336.
- [17] Yu FR, Xu B, Zhang JJ, Yu DL, He JL, Liu ZY, Tian YJ. Structural and thermoelectric characterizations of high pressure sintered nanocrystalline Bi_2Te_3 bulks. *Mater Res Bull*. 2012;47: 1432.

- [18] Wang SY, Xie WJ, Li H, Tang XF. High performance n-type (Bi, Sb)₂(Te, Se)₃ for low temperature thermoelectric generator. *J Phys D Appl Phys*. 2010;43(33):335404.
- [19] Pan Y, Li JF. Thermoelectric performance enhancement in n-type Bi₂(TeSe)₃ alloys owing to nanoscale inhomogeneity combined with a spark plasma-textured microstructure. *NPG Asia Mater*. 2016;8(6):e275.
- [20] Son JH, Oh MW, Kim BS, Park SD. Optimization of thermoelectric properties of n-type Bi₂(Te, Se)₃ with optimizing ball milling time. *Rare Met*. 2018;37(4):351.
- [21] Zhai RS, Wu YH, Zhu TJ, Zhao XB. Thermoelectric performance of p-type zone-melted Se-doped Bi_{0.5}Sb_{1.5}Te₃ alloys. *Rare Met*. 2018;37(4):308.
- [22] Duan XK, Hu KG, Ma DH, Zhang WN, Jiang YZ, Guo SC. Microstructure and thermoelectric properties of Bi_{0.5}Na_{0.02}Sb_{1.48-x}In_xTe₃ alloys fabricated by vacuum melting and hot pressing. *Rare Met*. 2015;34(11):770.
- [23] Chung DY, Iordanidis L, Choi KS, Kanatzidis MG. Complex chalcogenides as thermoelectric materials: a solid state chemistry approach. *Bull Korean Chem Soc*. 1998;19:1283.
- [24] Ji XH, He J, Su Z, Gothard N, Tritt TM. Improved thermoelectric performance in polycrystalline p-type Bi₂Te₃ via an alkali metal salt hydrothermal nanocoating treatment approach. *J Appl Phys*. 2008;104:034907.
- [25] Du BL, Li H, Tang XF. Enhanced thermoelectric performance in Na-doped p-type nonstoichiometric AgSbTe₂ compound. *J Alloys Compd*. 2011;509:2039.
- [26] Drašar Ć, Hovorková A, Lošťák Kong H, Li CP, Uher C. Figure of merit of quaternary (Sb_{0.75}Bi_{0.25})_{2-x}In_xTe₃ single crystals. *J Appl Phys*. 2008;104(023701):1.
- [27] Minnich AJ, Dresselhaus MS, Ren ZF, Chen G. Bulk nanostructured thermoelectric materials: current research and future prospects. *Energy Environ Sci*. 2009;2:466.
- [28] Sales BC, Mandrus D, Chakoumakos BC. Filled skutterudite antimonides: electron crystals and phonon glasses. *Phys Rev B*. 1997;56(23):15081.
- [29] Zhao LD, Dravid VP, Kanatzidis MG. The panoscopic approach to high performance thermoelectrics. *Energy Environ Sci*. 2014;7:251.
- [30] Chen ZW, Zhang XY, Pei YZ. Manipulation of phonon transport in thermoelectrics. *Adv Mater*. 2018;1705617:1.
- [31] Shen JJ, Fang T, Fu TZ, Xin JZ, Zhao XB, Zhu TJ. Lattice thermal conductivity in thermoelectric materials. *J Inorg Mater*. 2019;34(3):260.